

Identifying and interpreting spectral features of dissolved poly(dA)-poly(dT) DNA polymer in the high-microwave range

V. K. Saxena

Department of Physics, Purdue University, West Lafayette, Indiana 47907

B. H. Dorfman

Department of Physics, California State Polytechnic University, Pomona, California 91768

L. L. Van Zandt

Department of Physics, Purdue University, West Lafayette, Indiana 47907

(Received 24 September 1990)

The vibrational modes involving the hydrogen-bond fluctuations in *B* conformation of poly(dA)-poly(dT) DNA homopolymer dissolved in aqueous solution have been theoretically studied within the recently developed effective-field model, including longitudinal as well as radial fields, and a properly frequency-dependent dielectric constant for the surrounding water. We have analyzed the vibrational eigenvectors to characterize two types of motions involving hydrogen bonds, namely, propeller twist and hydrogen-bond breathing. We ran our analysis for five different sets of partial atomic charges, and found that the major mode frequencies are essentially independent of the choice of partial charges. Since hydrogen-bond strength changes with temperature, we simulated the effect of temperature on the hydrogen bonds by varying the hydrogen-bond force constants. Our calculations indicate that a mode near 42 cm^{-1} with strong propeller twist motion is to be expected. Around 63 cm^{-1} , another mode with strong hydrogen-bond breathing character should be found. We discuss the expected variations of these resonances with temperature as a guide to spectral identification.

I. INTRODUCTION

Two major types of dynamical motion strongly involving the hydrogen bonds in a DNA polymer have been identified. One is "propeller twist," defined as relative rotation of the two bases of a pair in opposite directions about the axis determined by the two base-sugar links. Structural studies of single-crystal DNA dodecamers have even revealed the presence of stable propeller twist static distortion for regions of crystallized DNA polymer containing numerous contiguous A-T base pairs.^{1,2} It has been suggested that these departures into the propeller twist conformation might arise in solution in accompaniment with softening of characteristic vibrational modes.³ The other major motion involving the hydrogen bonds is the so-called "breathing" motion in which the two bases oscillate in opposition, stretching and compressing the hydrogen bonds. These hydrogen bond breathing modes have even been supposed to offer a complete theory of DNA melting.^{4,5} We would certainly agree that such motions would be involved to an important extent in melting.

Recently Young, Prabhu, Prohofsky, and Edwards⁶ (hereafter YPPE) predicted modes with strong propeller twist lying in the range $43\text{--}53\text{ cm}^{-1}$. Their theory—actually eight different theories—show large variations for different sets of charges and different fittings for the various other nonbonding interactions. Despite the considerable variety of parameter sets used by YPPE, strong

propeller twist mode and a breathing mode tend to remain somewhere within this general high microwave frequency range.

We have previously published⁷ predictions concerning spectral lines of dissolved DNA polymer in the frequency range $10\text{--}200\text{ cm}^{-1}$. (See earlier references for details of structures, force constants, parameter values, etc.) This range is—as we have emphasized—particularly interesting for several reasons: tunable sources of sufficient power to penetrate watery material are currently being rapidly improved, the fundamental parameters of the atomic interactions in this range are poorly known, and the characteristic eigenvectors of the molecular vibrations are such as to be potentially more interesting for biology in this range than for either much higher or much lower ranges.⁸ Some spectroscopic data on films and fibers have been published,^{9,3,10} but information on well-dissolved polymers remains sparse.

Theory suggests that this frequency range should be fairly rich with spectral features.^{7,11,12} All models of DNA sufficiently detailed to refer to individual atoms show molecular resonances every 10 cm^{-1} or so; furthermore, DNA polymer is of low symmetry so that virtually none of the lines is truly forbidden either to IR or Raman spectroscopy. This plenitude of predictions becomes an impediment to progress, however, because we lack methods for determining which line is which. We do not know which observed line corresponds to which theoretical line, and, lacking this translational key, do not know

how to refine the parameters of the theory the better to correspond with molecular reality. Experimentally, *eigenvector* information is much scarcer than *eigenvalue* (frequency) information.

In the optical and near-infrared frequency range, characteristic vibrations are so localized that even eigenvector information is transferable from one molecular system to another. Spectroscopists can follow and identify a line by its relatively unchanged frequency and strength across a series of compounds. Even in the near infrared, however, this method may be dangerous, because of the tendency of the motion to spread out over much of a complex molecule.¹³ In the high microwave range we are discussing here, this method is completely hopeless.

We have elsewhere discussed the possibility of identifying eigenvectors by the method of isotopic substitution.¹⁴ This method requires an experimental ability to compare spectral lines with a precision of a few percent. The current state of experimental technique does not afford this kind of discrimination in this range. Such may well be a permanent feature of this range.

We are therefore led to seek other features by which we can identify the observed lines. The possibility we discuss here is the use of the temperature variation of the lines for identification. Specifically, several of the lines in this range are sensitive to the properties of the hydrogen bonds holding the double helix together. Since these properties are temperature dependent upon quite modest temperature elevation—the whole structure comes apart well below the boiling point of water—the temperature dependence of a spectroscopic frequency offers a means of matching it to its theoretical counterpart.

Good hydrogen-bond stretch force constants can be obtained from Lippincott-Schroeder potentials.^{15,16} Gao and co-workers^{17,18} have described the temperature dependence of these potentials based on a particular model of nonlinearity. As the temperature increases the hydrogen bonds should become more distended and softer. This should be reflected in certain modes showing dominant hydrogen-bond motion falling in frequency; the propeller twist and breathing modes should soften with $T \rightarrow T_{\text{melt}}$ where T_{melt} is the melting temperature of the double helix.

We here address the above points about the two major hydrogen-bond-related modes within the recent effective-field model developed by us for the nonbonded long-range interactions in DNA polymers.^{7,11,12} This model also includes explicitly the presence of the surrounding aqueous medium and the counterions, and accounts for the frequency dependence of the dielectric response of the system,¹² which is of considerable importance in this frequency range. Although these matters have been taken up before,⁶ we find it necessary to repeat these calculations for several reasons.

(1) The calculations of YPPE (Ref. 6) use a different parameter set for each distinct phenomenon considered. When fitting sound speed,¹⁹ dielectric constants of 81 and 6 were necessary. For higher-frequency waves, the value 81 was reduced to 9. An additional arbitrary factor of 1.8 was used to scale potentials in their first calculation.²⁰

In the second,^{5,6} all the charge values were arbitrarily reduced by a factor of 2.31 resulting in a reduction by 5.34 in all Coulombic interactions in the theory. A citation given to an x-ray experimental electron density measurement²¹ suggests the authors may have confused the neutral acid system of the x-ray crystals with the charged anion polymer of the theory, but under no supposition have we been able to reproduce the 2.31 factor.

(2) All the nonbonding interactions in their theory^{6,20} have been replaced by absolute values. For Coulomb interactions, this ansatz turns all charges positive. For van der Waals interactions, the long-range attractive parts are thereby made repulsive. In another publication,⁵ dealing with the melting problem, Coulomb and van der Waals terms are combined before the absolute value signs appear. In one of the calculations the van der Waals interaction term is reduced by a factor 1/15.4, in another it is reduced by $-1/38.5$.

(3) No valid arguments are adduced for any of these substitutions. In the most recent discussion⁶ all six models are presented on an equal footing, suggesting that all the predictions are of equal value.

We believe these manipulations have no physical basis. They therefore offer little guidance for experiments and have no predictive power. That they are necessary in the calculations of Refs. 5, 6, and 20 is a signal of the inability of the pairwise interaction model used there to simulate what actually occurs; an electromagnetic wave travels on the DNA and penetrates the surrounding medium as an inseparable component of the fundamental excitations of this charged, elastic system.

We have used our effective-field model^{7,11,12} to calculate and identify the eigenvectors of the modes with strong propeller twist using different choices for partial atomic charges. The partial charges on individual atoms are very difficult to measure. There are several relatively inconsistent sets of theoretically obtained partial charges in the literature.^{22–24} Hence we regard the partial charges as being very poorly known. In order for our calculations to be of any predictive value, it is necessary that our results be shown to be relatively insensitive to the inescapable ambiguity of the charges. This, fortunately, proves to be the case. Further, we have simulated the effect of temperature variation on the hydrogen bonds by reducing the strength of the hydrogen-bond force constants progressively. We have used the structure given by Chandrasekaran and Arnott^{25,26} taken from x-ray data of drawn fibers.

In the following section we review our effective-field approach for the nonbonded long-range interactions and present the parameter values used in our calculations for a poly(dA)-poly(dT) homopolymer. In view of the history of such calculations as these, it should be noted that our theory contains no freely adjustable parameters. All constants are obtained from other sources or confined by physical reasonableness to narrow ranges. Section III contains the results of our calculations for exploring the effect of partial charges on the two major hydrogen-bond modes, i.e., the propeller twist mode and the breathing mode, for five different sets of partial atomic charges. In Sec. IV we present the results of our calculation to simu-

late the effect of temperature on the hydrogen-bond strengths and the consequent variations of the frequencies of the modes in the high microwave range. Finally, the last section contains conclusions and a discussion of our calculations.

II. MODEL FOR DISSOLVED DNA POLYMER

Dynamics of a DNA polymer dissolved in water solution are described by the set of equations of motion for the DNA-water sheath system^{11,12}

$$-\omega^2 q_i^\alpha = \sum_{j,\beta} D_{ij}^{\alpha\beta} q_j^\beta + \acute{e}_i E_\alpha - i\omega \Gamma_i (\bar{s} - q_i^\alpha \eta_i) \delta_{iP} \delta_{\alpha z} \quad (1)$$

and

$$-\omega^2 \bar{s} = -q^2 v_w^2 \bar{s} - \lambda E_z - i\omega \sum_i \Gamma_i (q_i^z - \bar{s} / \eta_i) \delta_{iP} - i\dot{\gamma} \omega \bar{s}, \quad (2)$$

where ω is a frequency of a mode of the system. q_i^α is the α ($=x, y, z$) component of the mass-weighted displacement amplitude vector \mathbf{q}_i of atom i , defined by $\mathbf{q}_i = \sqrt{m_i} \delta \mathbf{r}_i$, with mass m_i and the corresponding coordinate \mathbf{r}_i . $\bar{s} = s\sqrt{a\rho}$ where s represents the displacement amplitude of the near water sheath containing the counterions, ρ is the linear mass density of the sheath, and a is the helix rise. We have assumed only longitudinal motion of the counterion-water sheath. The first term on the right of Eq. (1) contains part of the dynamical matrix which arises, within the harmonic approximation, from the bonded interactions resulting from bond stretch, angle bend, and twist. This term also contains the Coulomb forces between partial atomic charges within a unit cell, and also includes the van der Waals forces between pairs of atoms within the central cell and the nearest-neighbor cells. Collection of all these forces is contained in the force-constant matrix $D_{ij}^{\alpha\beta}$. As in our recent publications,^{11,12} unlike the refinements of YPPE,⁶ in the Coulomb and van der Waals parts of the force-constant matrix the atomic partial charges and the other parameters appear with their proper algebraic signs, and no absolute values are used.

The last term on the right of Eq. (1) represents the dissipative force at the polymer-solvent interface, with a similar term in Eq. (2), the equation of motion for the water-counterion sheath. Equation (2) also contains the term $-i\omega\dot{\gamma}\bar{s}$ for damping at the sheath-bulk-water interface. The first term on the right-hand side of Eq. (2) represents the elastic contribution to the sheath motion, v_w being the sound speed in bulk water, and q the wave vector for propagation of the disturbance along the DNA-solvent system; $\eta_i \equiv \sqrt{a\rho/m_i}$. Kronecker deltas δ_{iP} and $\delta_{\alpha z}$ restrict the frictional forces between the DNA and the water sheath to the coupling of the z component of the motion of phosphorus atoms on the two backbones with longitudinal motion of the sheath. The damping parameter $\dot{\gamma}$, for the sheath-bulk-water coupling, is derived from bulk water.²⁷

The nonbonded, long-range interactions between distant parts of the polymer are accounted for in terms of

the effective local electric field^{11,12} \mathbf{E} with components E_α coupled to the atomic partial charges on the polymer and to the net counterion charge within the sheath. In Eqs. (1) and (2) the local field terms contain the scaled charges $\acute{e}_i = e_i / \sqrt{m_i}$ where e_i is the partial charge on atom i . $\lambda = \lambda / \sqrt{a\rho}$ with $-\lambda = -\sum_i e_i$ being the total charge of the counterions within the water sheath. We have assumed complete charge neutrality within the molecule-sheath system. Poisson-Boltzmann theory indicates that this is correct to about 5%.

At the limit of infinite dilution, the local effective electric field \mathbf{E} is related to the local electric polarization density \mathbf{P} by the relation¹¹

$$\mathbf{E}(\omega) = \frac{1}{\epsilon_{\text{in}}} \frac{\hat{\mathbf{r}} F(\kappa, \omega) P_r + \hat{\mathbf{z}} P_z}{F(\kappa, \omega) - 1}, \quad (3)$$

where

$$F(\kappa, \omega) = \frac{i\sigma + \omega\epsilon_{\text{out}}(\omega)}{\omega\epsilon_{\text{in}}} \frac{2}{\kappa r_1} \frac{H_1^1(\kappa r_1)}{H_0^1(\kappa r_1)}. \quad (4)$$

P_r and P_z are the radial and longitudinal components, respectively, of the polarization density vector \mathbf{P} . r_1 is the radius of the cylinder defining the molecule-sheath system. H_0^1 and H_1^1 are zeroth- and first-order Hankel functions of first kind, and σ is the dc electrical conductivity of the solvent. ϵ_{in} is the average dielectric constant within the cylindrical region of the DNA and the water sheath. $\epsilon_{\text{out}}(\omega)$ is the dielectric constant of the surrounding solvent medium. κ is a function of ω , σ , and the wave vector q given by

$$\kappa^2 = -(q^2 - \epsilon_{\text{out}} \mu_0 \omega^2 - i\sigma \mu_0 \omega), \quad (5)$$

where μ_0 is the well-known constant of magnetostatics. The local electric polarization density \mathbf{P} is given by

$$\mathbf{P} = \frac{1}{\pi r_1^2 a} \left[\sum_i e_i \delta \mathbf{r}_i - \hat{\mathbf{z}} s \lambda \right]. \quad (6)$$

In our earlier calculations^{11,12} we coupled the partial atomic charges only to the longitudinal part E_z of the local electric field. To be more complete in the present calculation we have also included the small radial contribution E_r of the local effective field in the dynamical matrix. The frequency-dependent dielectric function of the medium $\epsilon_{\text{out}}(\omega)$ is given by²⁸

$$\epsilon_{\text{out}}(\omega) = \frac{\epsilon_{\text{dc}} - \epsilon_\infty}{1 + i\omega\tau_s} + \epsilon_\infty, \quad (7)$$

where ϵ_{dc} and ϵ_∞ are the zero-frequency static dielectric constant and infinite frequency dielectric constant of the aqueous medium, respectively. τ_s is the dielectric relaxation time of the solvent medium, taken to be 7.9×10^{-12} sec from the most recent value reported from microwave absorption measurements.²⁹ This places the range of most rapid variation of ϵ_{out} around 50–100 cm^{-1} .

The frequency dependence of the local field terms and the damping terms turns the set of equations (1) and (2) nonlinear in ω^2 and makes them difficult to solve by direct diagonalization. We calculated the spectrum of

B-form poly(dA)-poly(dT) DNA within this model using an iterative procedure to get self-consistent eigenmode frequencies and corresponding eigenvectors for each of the modes separately. For the frequency-independent parts of the force constant matrix $D_{ij}^{\alpha\beta}$, the damping coefficients, the sound speed for bulk water, and the values of σ and r_1 in the effective-field terms we used the same set of values as in our earlier calculation.¹² Brillouin scattering studies of DNA and its hydration shell³⁰ show that the dielectric relaxation time within the first hydration shell is 4.0×10^{-11} sec. In accord with this in Eq. (3) we have used a value of $2.0\epsilon_0$ for ϵ_{in} , the dielectric permittivity of the cylindrical region containing the DNA helix and the primary hydration sheath. In Eq. (6) for ϵ_{dc} we have used a value of $68.0\epsilon_0$ corresponding to water with a counterion concentration³¹ of about 15%. ϵ_∞ was taken to be $1.77\epsilon_0$.

III. PARTIAL ATOMIC CHARGES AND HYDROGEN-BOND MODES

For different sets of partial atomic charges the calculations of YPPE (Ref. 6) show large variations in the frequency of the mode with strongest propeller twist. In order to examine this fact we ran the calculation described in the last section for a poly(dA)-poly(dT) homopolymer in the *B* conformation for five different sets of partial atomic charges. We analyzed the eigenvectors of the modes in the high microwave range in order to identify the modes with strongest propeller twist and hydrogen-bond breathing characters. These characteristics were identified by analyzing and examining the eigenvectors in terms of standard vectors for these motions. The propeller twist is defined as the relative angular rotation, in opposite directions, of the average planes of the bases about the long axis determined by the two nitrogen-carbon bonds connecting the bases to their respective sugars. The magnitude of the projection of an eigenvector on to the standard vector for a unit propeller twist gives the fractional amount of propeller twist motion contained in the particular mode being examined. Similarly the analysis of displacements of the bases in opposite directions along the same long axis defined above, stretching the hydrogen bonds, determines the breathing character. We represent these quantities by ψ_{PT} for propeller twist and by d_{HB} for hydrogen-bond stretch.

We used the partial atomic charges from modified intermediate neglect of differential overlap (MINDO3) calculations of Miller,²³ charges of Renugopalkrishnan, Lakshminarayanan, and Sasisekharan²² (RLS), and the *ab initio* charges determined by Nuss and Kollman²⁴ (NK). (We did not reduce the Miller charges by the arbitrary factor of 2.31.⁶) In this context it should be noted that each of these three sets of partial charges gives approximately the same value for the total charge on the anionic polymer unit cell containing a base pair and corresponding ribose-phosphate backbones. The Miller charges give a value of -1.93 (in units of electronic charge); the RLS charges give a value of -1.99 ; and NK charges give -1.86 . (Miller charges reduced by 2.31 lead to a total charge of -0.84 which is only about 21% of

TABLE I. Values of propeller twist frequency ω_{PT} , fractional propeller twist ψ_{PT} , breathing mode frequency ω_{HB} , and fractional hydrogen-bond stretch d_{HB} of a poly(dA)-poly(dT) homopolymer at the zone center $\theta=0^\circ$ for five different sets of partial atomic charges. ω is in cm^{-1} .

Charges	ω_{PT}	ψ_{PT}	ω_{HB}	d_{HB}
Miller	42.56	0.5218	61.57	0.5932
NK	42.25	0.5413	61.70	0.5952
RLS	42.05	0.5238	61.58	0.5920
M-NK	42.55	0.5374	61.70	0.5925
NK-RLS	42.20	0.5402	61.72	0.5963

the expected total charge.) Based on x-ray determination of partial atomic charges, Pearlman and Kim²¹ have argued that the NK charges are closest to the experimentally determined charges in the sugar and base regions, while the RLS charges match best in the phosphate region. Based on this argument we also used two other sets of partial charges. In one the Miller charges were used for the sugar and phosphate backbones and NK charges were used for the bases (we call this set the M-NK set). Another set was formed by using the RLS charges for the phosphate group atoms and NK charges for the sugar and base regions, and call it NK-RLS charges.

We ran our calculations for the above five sets of charges for two values of the phase angle θ ($=qa$), that is, for the longitudinal excitations at $\theta=0^\circ$ and for transverse excitations at $\theta=36^\circ$. Our results are presented in Tables I and II for these two cases. In these tables we display the frequency ω_{PT} of the mode showing the strongest propeller twist, the fractional propeller twist ψ_{PT} for this mode, the frequency ω_{HB} for the mode with strongest hydrogen-bond breathing character, and the corresponding fractional hydrogen-bond stretch d_{HB} for all five sets of partial charges.

From Tables I and II one can see that the four quantities displayed show very little variation for different sets of partial charges. For comparison the propeller twist mode frequency ω_{PT} shows a variation only of the order of 2% among the five sets of charges, in contrast to the case of YPPE (Ref. 6) who found variations of about 20% for this frequency for different charges and refinements. Similarly the other three quantities remain almost unchanged for different choices of partial atomic charges. We also examined the variation of frequencies of other modes (not listed here in tables), in the high microwave range, with similar eigenvector characteristics or showing

TABLE II. Same as Table I for $\theta=36^\circ$.

Charges	ω_{PT}	ψ_{PT}	ω_{HB}	d_{HB}
Miller	42.13	0.6998	62.06	0.5371
NK	41.82	0.6655	61.94	0.5460
RLS	41.61	0.6508	61.95	0.5462
M-NK	41.80	0.6838	61.97	0.5435
NK-RLS	41.68	0.6555	63.15	0.4960

relatively weaker fractional propeller twist and fractional breathing characters. These modes also showed similar behavior as shown by modes with strong propeller twist or breathing character, and the frequencies of all these modes practically remained unchanged for different sets of partial charges used in this investigation.

IV. TEMPERATURE EFFECT ON HYDROGEN-BOND MODES

As mentioned in the Introduction temperature variation of the mode frequencies can be used as a means for identifying the experimentally observed data. It is known that the hydrogen-bond force constants depend on the variations in temperature.^{17,18} Therefore, to simulate the effect of temperature on the spectral features we performed our iterative calculation of the eigenfrequencies and eigenvectors on a number of different sets of hydrogen-bond force constants. We define the relative strength of the hydrogen bond Δ_{HB} as the strength measured in terms of full hydrogen-bond strength at room temperature. Corresponding to the general weakening with rising T , an increase in Δ_{HB} means lowering of temperature, whereas a decrease in Δ_{HB} corresponds to an increase in temperature. We ran our calculations for higher as well as lower temperatures. For this purpose we chose values of Δ_{HB} ranging from 1.4 to 0.1. A value of 1.0 for Δ_{HB} corresponds to the full strength at room temperature. Once again we ran our calculations both for longitudinal- as well as transverse-polarized excitations, i.e., for $\theta=0^\circ$ and 36° . Our results for these angles are presented in Tables III and IV.

From Tables III and IV one can clearly see that the frequencies of two of the modes fall, as expected, with increasing temperature (decreasing Δ_{HB}). The frequency of the mode with strongest propeller twist ω_{PT} and the related fractional twist ψ_{PT} are relatively slowly varying functions of temperature. On the other hand, the frequency of the breathing mode ω_{HB} and the corresponding relative hydrogen-bond stretch d_{HB} are found to be very sen-

TABLE III. Variation of propeller twist frequency ω_{PT} , fractional propeller twist ψ_{PT} , breathing mode frequency ω_{HB} , and fractional hydrogen bond stretch d_{HB} with temperature (represented in terms of reduced hydrogen-bond strength) of a poly(dA)-poly(dT) homopolymer at the zone center $\theta=0^\circ$. In the first column the numbers represent the relative strength Δ_{HB} of hydrogen bonds in terms of full strength used for the calculations in Sec. III. ω is in cm^{-1} .

Δ_{HB}	ω_{PT}	ψ_{PT}	ω_{HB}	d_{HB}
1.4	42.63	0.5307	64.54	0.4876
1.2	42.60	0.5307	63.24	0.5344
1.0	42.56	0.5218	61.57	0.5932
0.8	42.52	0.5313	59.28	0.6692
0.6	42.46	0.5313	55.88	0.7671
0.4	42.33	0.5320	50.35	0.8769
0.2	43.15	0.4020	39.49	0.5647
0.1	42.70	0.4985	25.03	0.5479

TABLE IV. Same as Table III for $\theta=36^\circ$.

Δ_{HB}	ω_{PT}	ψ_{PT}	ω_{HB}	d_{HB}
1.4	42.21	0.6938	64.84	0.4507
1.2	42.18	0.6967	63.62	0.4904
1.0	42.13	0.6998	62.06	0.5371
0.8	42.09	0.7032	59.95	0.5854
0.6	42.03	0.7075	56.99	0.5923
0.4	41.93	0.7133	49.93	0.6673
0.2	42.67	0.4673	40.07	0.5285
0.1	42.17	0.6639	26.80	0.6464

sitive to temperature variations. As the temperature increases the hydrogen bonds soften and it becomes easier to stretch the bonds. The breathing mode frequency decreases and the bond stretch increases.

One peculiar feature appears in the last two rows of Tables III and IV. First the frequency of the propeller twist mode for $\Delta_{\text{HB}}=0.2$ is higher than that for $\Delta_{\text{HB}}=0.4$ contrary to the expected decrease. Also the fractional twist ψ_{PT} and bond stretch d_{HB} for the value $\Delta_{\text{HB}}=0.2$ are found to be lower than the respective values for $\Delta_{\text{HB}}=0.4$. Carefully examining various modes around the high microwave range and their eigenvector characteristics one finds that besides the modes with strongest propeller twist or breathing characters there are other modes with relatively weaker characteristics of these types. Particularly at $\theta=0^\circ$ for $\Delta_{\text{HB}}=0.2$ the propeller twist and breathing characters are mixed and are distributed among three nearby modes. These modes lie at 36.22, 39.49, and 43.15 cm^{-1} . The corresponding fractional twist component for these modes are found to be 0.2079, 0.2374, and 0.4020. The related hydrogen-bond stretches for the same modes turn out to be 0.1459, 0.5647, and 0.2521, respectively. For $\Delta_{\text{HB}}=0.1$ the breathing character is shared by two adjacent modes at 25.03 and 32.72 cm^{-1} ; and the propeller twist is shared by the adjacent modes at 36.78 and 42.70 cm^{-1} .

Similarly at $\theta=36^\circ$ and for $\Delta_{\text{HB}}=0.2$ the propeller twist and breathing characteristics are distributed over different modes. The propeller twist and breathing characters are shared by both modes at 40.07 and 42.67 cm^{-1} with the related ψ_{PT} values of 0.3063 and 0.4673, respectively. The hydrogen-bond stretches for these modes are found to be 0.5285 and 0.2397, respectively. A mode at 85.94 cm^{-1} shows relatively weaker propeller twist character with $\psi_{\text{PT}}=0.2274$; and a mode at 30.16 cm^{-1} has a weak hydrogen bond stretch $d_{\text{HB}}=0.1267$.

Even for $\Delta_{\text{HB}}=1.0$ also there are modes, other than listed in Tables III and IV, some with relatively weaker propeller twist or breathing character. For example, at $\theta=0^\circ$ a mode at 36.63 cm^{-1} shows a propeller twist $\psi_{\text{PT}}=0.2847$, and a mode at 106.51 cm^{-1} has a significant hydrogen-bond stretch $d_{\text{HB}}=0.3174$. At $\theta=36^\circ$, the related mode at 107.22 cm^{-1} shows a hydrogen-bond stretch $d_{\text{HB}}=0.3174$. Like the principal modes with strong breathing characteristics, these modes also show much sensitivity to temperature variations. It appears that the mode around 106 cm^{-1} for $\Delta_{\text{HB}}=1.0$

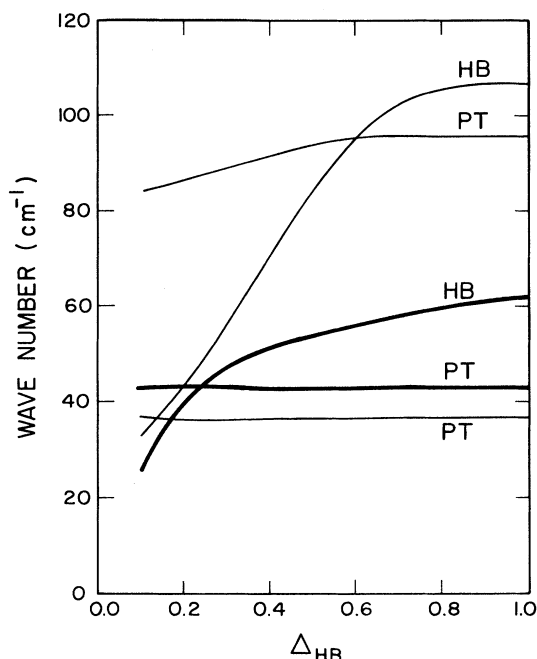


FIG. 1. Variation of frequency ω as a function of Δ_{HB} at $\theta=0^\circ$ for some modes showing fractional propeller twist (PT) or hydrogen-bond breathing (HB) characters. Thicker lines correspond to modes with strongest PT or HB characteristics.

softens to a mode with similar eigenvector characteristics around 43 cm^{-1} for $\Delta_{\text{HB}}=0.2$ and to a mode around 32 cm^{-1} for $\Delta_{\text{HB}}=0.1$. We have displayed the variation of frequencies of some important modes discussed above as a function of Δ_{HB} for $\theta=0^\circ$ in Fig. 1. Curves marked PT show a fractional propeller twist, whereas the curves marked HB are for the modes showing substantial hydrogen breathing character.

V. DISCUSSION

In this paper we have offered the possibility of identifying and interpreting mode characteristics of the vibrational spectrum of a poly(dA)-poly(dT) homopolymer in the high microwave range. We utilized our most recent effective-field approach for the inclusion of long-range nonbonded interactions. We would like to emphasize that we did not use any parameter fitting, artificial, and unphysical absolute value signs, or any unphysical scale factors. All our parameters, except the dielectric con-

stant of the inner sheath $2\epsilon_0$, were taken either from existing experimental data or from established theoretical values. As already shown elsewhere^{7,12} our model is able to reproduce the existing experimental data, within the limits of applicability to infinitely dilute solution, within this single set of parameter values. We attribute this success to including the effect of surrounding aqueous medium and the counterions on the vibrational dynamics of the polymer in the theory.

We have examined the dependence of mode frequencies in the high microwave range, on the choice of partial atomic charges used in the long-range part of the nonbonded interactions. We found that the frequencies of the modes, not only in the high microwave range but also of the modes in the millimeter microwave range, are insensitive to the choice of partial charges. As pointed out earlier, a scale factor 2.31 used by YPPE for Miller charges is not physical and is unnecessary.

We also studied the effect of temperature on the modes, in terms of gradually decreasing hydrogen-bond strengths. We point out that such a variation of mode frequencies with temperature may possibly be used as a means of identifying the characteristic eigenvectors associated with the modes. We observe that the effect of temperature, as is also expected, is most prominent on modes with hydrogen-bond stretching or breathing characters. The modes with propeller twist show relatively weaker dependence on temperature. It should be realized that a more profound analysis of eigenvectors and corresponding variation of mode frequencies, for example, other types of subunit motions,⁸ might possibly give more insight into the problem of identifying eigenvector characteristics of vibrational modes in the low to medium frequency range. The temperature variation of each of the frequencies with similar eigenvector characteristics should turn out to be an easier way to identify the modes.

ACKNOWLEDGMENTS

The work at Purdue University was performed under the Office of Naval Research (ONR), Contract No. N00014-87-K-0162 funded by the Strategic Defense Initiative Organization. The work at California State Polytechnic University (CALPOLY) was partly supported by Numerix Division of the Mercury Corporation, GTE Foundation Grant of Research Corporation, and Research Scholarship and the Creative Activities program of CALPOLY. One of us (B.H.D.) acknowledges the release time made available to him by the College of Science, CALPOLY.

¹H. C. M. Nelson, J. T. Finch, B. F. Luisi, and A. Klug, *Nature* (London) **330**, 221 (1987).

²M. Coll, C. A. Frederick, A. J. H. Wang, and A. Rich, *Proc. Natl. Acad. Sci. U.S.A.* **84**, 8385 (1987).

³C. Liu, G. S. Edwards, S. Morgan, and E. Silberman, *Phys. Rev. A* **40**, 7394 (1989).

⁴Y. Kim, K. V. Devi-Prasad, and E. W. Prohofsky, *Phys. Rev. B* **32**, 5185 (1985).

⁵V. V. Prabhu, L. Young, and E. W. Prohofsky, *Phys. Rev. B* **39**, 5436 (1989).

⁶L. Young, V. V. Prabhu, E. W. Prohofsky, and G. S. Edwards, *Phys. Rev. A* **41**, 7020 (1990).

- ⁷L. L. Van Zandt and V. K. Saxena, *Phys. Rev. A* **39**, 2672 (1989).
- ⁸V. K. Saxena, L. L. Van Zandt, and W. K. Schroll, *Chem. Phys. Lett.* **164**, 82 (1989).
- ⁹J. W. Powell, G. S. Edwards, L. Genzel, F. Kramer, A. Wittlin, W. Kubasek, and W.L. Peticolas, *Phys. Rev. A* **35**, 3929 (1987).
- ¹⁰T. Weidlich, S. M. Lindsay, Qi Rui, A. Rupprecht, W. L. Peticolas, and G. A. Thomas, *J. Biomol. Struct. Dynam.* **8**, 139 (1990).
- ¹¹V. K. Saxena, L. L. Van Zandt, and W. K. Schroll, *Phys. Rev. A* **39**, 1474 (1989).
- ¹²V. K. Saxena and L. L. Van Zandt, *Phys. Rev. A* **42**, 4993 (1990).
- ¹³K.-C. Lu, L. L. Van Zandt, and E. W. Prohofsky, *Biophys. J.* **28**, 27 (1979).
- ¹⁴L. L. Van Zandt and V. K. Saxena, *Biopolymers* **30**, 87 (1990).
- ¹⁵E. R. Lippincott and R. Schroeder, *J. Chem. Phys.* **23**, 1099 (1955).
- ¹⁶R. Schroeder and E. R. Lippincott, *J. Phys. Chem.* **61**, 921 (1957).
- ¹⁷Y. Gao and E. W. Prohofsky, *J. Chem. Phys.* **80**, 2242 (1984).
- ¹⁸Y. Gao, K. V. Devi-Prasad, and E. W. Prohofsky, *J. Chem. Phys.* **80**, 6921 (1984).
- ¹⁹M. B. Hakim, S. M. Lindsay, and J. Powell, *Biopolymers* **23**, 1185 (1984).
- ²⁰V. V. Prabhu, W. K. Schroll, L. L. Van Zandt, and E. W. Prohofsky, *Phys. Rev. Lett.* **60**, 1587 (1988).
- ²¹D. A. Pearlman and S. H. Kim, *Biopolymers* **27**, 327 (1985).
- ²²V. Renugopalkrishnan, A. V. Lakshminarayanan, and V. Sasisekharan, *Biopolymers* **10**, 1159 (1971).
- ²³K. J. Miller, *Biopolymers* **18**, 959 (1979).
- ²⁴M. E. Nuss and P. A. Kollman, *J. Med. Chem.* **22**, 1517 (1979).
- ²⁵R. Chandrasekaran and S. Arnott, in *Numerical Data and Functional Relationship in Science and Technology*, edited by W. Saenger, Landolt-Börnstein, New Series, Group VII, Vol. 1, pt. b (Springer-Verlag, Berlin, 1989).
- ²⁶S. Arnott, R. Chandrasekaran, A. K. Banerjee, R. He, and J. K. Walker, *J. Biomol. Struct. Dynam.* **1**, 437 (1983).
- ²⁷B. H. Dorfman and L. L. Van Zandt, *Biopolymers* **23**, 913 (1984).
- ²⁸R. Pethig, *Dielectric and Electronic Properties of Biological Materials* (Wiley, New York, 1979).
- ²⁹H. R. Garner, A. C. Lewis, and T. Ohkawa (unpublished).
- ³⁰N. J. Tao, S. M. Lindsay, and A. Rupprecht, *Biopolymers* **27**, 1655 (1988).
- ³¹J. B. Hubbard, L. Onsager, W. M. Van Beek, and M. Mandel, *Proc. Natl. Acad. Sci. U.S.A.* **74**, 401 (1977).